# Optimal Control of a Qubit Coupled to a Non-Markovian Environment

P. Rebentrost,[1,2,3,*] I. Serban,[1,2] T. Schulte-Herbrüggen,[4] and F. K. Wilhelm[2,†]

[1]*Department Physik, ASC and CeNS, Ludwig-Maximilians-Universität, Theresienstrasse 37, 80333 München, Germany*
[2]*IQC and Department of Physics and Astronomy, University of Waterloo, 200 University Ave W, Waterloo, ON, N2L 3G1, Canada*
[3]*Department of Chemistry & Chemical Biology, Harvard University, 12 Oxford Street, Cambridge, Massachusetts 02138, USA*
[4]*Department of Chemistry, Technische Universität München, Lichtenbergstrasse 4, 85747 Garching, Germany*

(Received 26 January 2007; published 2 March 2009)

A central challenge for implementing quantum computing in the solid state is decoupling the qubits from the intrinsic noise of the material. We investigate the implementation of quantum gates for a paradigmatic, non-Markovian model: a single-qubit coupled to a two-level system that is exposed to a heat bath. We systematically search for optimal pulses using a generalization of the novel open systems gradient ascent pulse engineering algorithm. Next to the known optimal bias point of this model, there are optimal pulses which lead to high-fidelity quantum operations for a wide range of decoherence parameters.

DOI: 10.1103/PhysRevLett.102.090401 PACS numbers: 03.65.Yz, 02.30.Yy, 03.67.Lx, 85.25.Cp

A promising class of candidates for the practical realization of scalable quantum computers are solid-state quantum devices based on superconductors [1–5] and lateral quantum dots [6]. A key challenge to overcome in this enterprise is the decoherence induced by the coupling to the macroscopic bath of degrees of freedom not used for quantum computation (see, e.g., Ref. [7] for a review). Many of these decoherence sources can be engineered at the origin. In the case of intrinsic slow noise originating from two-level fluctuators (TLFs) this is much harder [8,9], albeit not impossible [10,11]. In order to advance the limitations of coherent quantum manipulations in the solid state, it is imperative to find strategies which accommodate this kind of noise. A number of methods have been proposed by intuition and analogies to different areas, such as dynamical decoupling [12,13], the optimum working point strategy [1,5,14], and NMR-like approaches [15]. Even in light of their success, it is by no means clear whether even better strategies can be formulated and, on a more general level, where the limits of quantum control under hostile conditions are reached.

We resort to numerical methods of optimal control. The closed systems GRAPE (gradient ascent pulse engineering) algorithm [16] has been proven useful in spin and pseudospin systems [17], an important example of the latter being coupled Josephson devices [18]. It was extended to open Markovian systems [19]. Other recent optimal control results also include the presence of noise and decoherence. Pure dephasing was considered in [20]. Reference [21] treated a semiclassical random-telegraph noise (RTN) model in the high-temperature limit, while [22] focussed on two qubits and classical $1/f$ noise. Optimal state transfer in the spin-boson model was considered in [23]. Reference [24] optimized qubit gates in the presence of finite-dimensional, dissipation-free environments. In this Letter, we generalize the GRAPE algorithm to include a complex environment leading to non-Markovian qubit dynamics and non-Gaussian noise. We show that next to an optimal working point there is also an optimal pulse shape and gate duration. Accelerating the fluctuations can improve the gate fidelity. We discuss the physics ultimately limiting the gate performance no longer correctable by pulse shaping.

*Model and method.*—In macroscopic samples, $1/f$ noise [8,9,25] occurs in most observables. The Dutta-Horn model [26,27] explains this phenomenon by the (classical) superposition of TLFs which randomly jump between their states, a process known as random-telegraph noise (RTN). In small, clean samples the discrete nature of the noise process from a single dominating fluctuator [1,28] can be resolved. This leads to semiphenomenological Hamiltonians [29–31].

We specifically model a qubit coupled to a single TLF by $H = H_S(t) + H_I + H_B$. $H_S$ consists of the qubit, defined by the states $|0\rangle$ and $|1\rangle$, and the coupled two-state system, i.e.,

$$H_S(t) = E_1(t)\sigma_z + \Delta\sigma_x + E_2\tau_z + \Lambda\sigma_z\tau_z. \qquad (1)$$

The Pauli matrices $\sigma_i$ and $\tau_i$ operate in qubit and fluctuator Hilbert space, respectively. $E_1(t)$ is time dependent and serves as an external control, while $\Delta$ is the static qubit tunnel splitting. $E_2$ is the TLF splitting and $\Lambda$ is the qubit-TLF coupling strength. The source of decoherence is the coupling of the fluctuator to the heat bath (described by bosonic operators $b_i$), which leads to incoherent transitions between the fluctuator eigenstates,

$$H_I = \sum_i \lambda_i(\tau^+ b_i + \tau^- b_i^\dagger), \qquad H_B = \sum_i \hbar\omega_i b_i^\dagger b_i. \qquad (2)$$

The $\tau^\pm$ are TLF raising or lowering operators. We introduce an Ohmic bath spectrum $J(\omega) = \sum_i \lambda_i^2 \delta(\omega - \omega_i) = \kappa\omega\Theta(\omega - \omega_c)$ containing the couplings $\lambda_i$, the dimensionless damping $\kappa$, and a high-frequency cutoff $\omega_c$ (which we assume to be the largest frequency in the system).

The dynamics of the combined qubit ⊗ TLF system is described by a master equation for the density matrix with

 

the bath traced out along the lines of [7,32]. In the motional narrowing regime $k_B T > \kappa E_2$, one arrives at the Bloch-Redfield equation

$$\dot{\rho}(t) = \frac{1}{i\hbar}[H_S, \rho(t)] + [\tau^+, \Sigma_1^- \rho(t)] + [\tau^-, \Sigma_0^+ \rho(t)] - [\tau^-, \rho(t)\Sigma_1^+] - [\tau^+, \rho(t)\Sigma_0^-] \quad (3)$$

with the different rate tensors ($s = 0, 1$)

$$\Sigma_s^{\pm} = \frac{1}{(i\hbar)^2} \int_0^\infty dt' \int_0^\infty d\omega J(\omega)(n(\omega) + s) e^{\pm i\omega t'} \tau^{\pm}(t'). \quad (4)$$

Here, $n(\omega)$ is the Bose function. The rate tensors explicitly depend on the control $E_1(t)$ due to the interaction representation of the operators $\tau^{\pm}$ in Eq. (4). Since tracing out the TLF at this stage would lead to an intricate non-Markovian master equation, we treat the qubit-TLF interactions exactly; i.e., the rate tensors act on the combined qubit-TLF system.

Our model goes far beyond a simple RTN noise model [13] and captures the correlations between qubit and TLF [29,31]. Still, it is useful to introduce the parameters of the RTN which would result for $\Lambda \to 0$. The TLF flipping rate is $\gamma = 2\kappa E_2 \coth(E_2/k_B T)$, the sum of the excitation and relaxation rate. It enters the two-point noise spectrum of random-telegraph noise

$$S(\omega) = \int_{-\infty}^{\infty} dt e^{-i\omega t} \langle \tau_z(t)\tau_z(0)\rangle_{\rm eq} = \Lambda^2 \frac{\gamma}{\omega^2 + \gamma^2}. \quad (5)$$

This is the Fourier transform of the interaction representation of $\tau_z$ assuming the bath in equilibrium. In this limit, one can find relaxation rates $1/T_1 = \frac{\Delta^2}{E^2} S(2E)$ and $1/T_2 = \frac{1}{2T_1} + \frac{E_1^2}{E^2} S(0)$ with $E = \sqrt{\Delta^2 + E_1^2}$. In [5] it was shown that pure dephasing can be suppressed by keeping $|E_1| \ll \Delta$ during all manipulations, the optimum working point strategy. Moreover, in the slow flipping regime, $1/T_1$ relaxation is small since $S(2\Delta) \simeq \Lambda^2\gamma/(4\Delta^2)$.

We formulate the control approach by rewriting Eq. (3) as $\dot{\rho}(t) = -(i\mathcal{H}(E_1(t)) + \Gamma(E_1(t)))\rho(t)$ with the Hamiltonian superoperator $\mathcal{H}(E_1(t))(\cdot) = \frac{1}{\hbar}[H_S(E_1(t)), \cdot]$ and the relaxation superoperator $\Gamma$, both time-dependent via the control $E_1(t)$. The formal solution to the master equation is a linear quantum map operating on a physical initial state according to $\rho(t) = F(t)\rho(0)$. $F$ itself follows the operator equation of motion

$$\dot{F} = -(i\mathcal{H} + \Gamma)F \quad (6)$$

with initial condition $F(0) = \mathbb{1}$, as in Ref. [19]. Here, multiplication of quantum maps denotes their concatenation. The task is to find control amplitudes $E_1(t)$ with $t \in [0, t_g]$, $t_g$ being a fixed final time, such that the difference $\delta F = F_U - F(t_g)$ between dissipative time evolution $F(t_g)$ obeying Eq. (6) and a target unitary map $F_U$ is minimized with respect to the Euclidean distance $\|\delta F\|_2^2 \equiv \mathrm{tr}\{\delta F^\dagger \delta F\}$. Maximizing the trace fidelity

$$\phi = \frac{1}{D^2} \mathrm{Re}\,\mathrm{tr}\{F_U^\dagger F(t_g)\} \quad (7)$$

is equivalent, where $D$ is the dimension of the Hilbert space. In an open system, one cannot expect to achieve zero distance to a unitary evolution $F_U$ [19]. The goal is to come as close as possible.

We find the pulses by a numerical gradient search. The quantum map is digitized, $F(t_g) \approx F_N \cdots F_j \cdots F_1$, where the interval $[0, t_g]$ is divided into $N$ slices of duration $\Delta t$. One finds by Eq. (6) that $F_j = \exp(-i\mathcal{H}[E_1(j)]\Delta t - \Gamma[E_1(j)]\Delta t)$, with $E_1(j)$ being the control amplitude in the $j$th time slice. The gradient of the fidelity can be computed in closed form as $\frac{\partial\phi}{\partial E_1(j)} = -\mathrm{Re}\,\mathrm{tr}\left\{F_U^\dagger F_N \cdots F_{j+1} \Delta t \frac{\partial(i\mathcal{H}(E_1(j)) + \Gamma(E_1(j)))}{\partial E_1(j)} F_j \cdots F_1\right\}$.

We aim at optimizing the evolution of the qubit alone. The TLF is traced out at the end of the full time evolution $F(t_g)$ retaining all degrees of freedom in the intermediate steps $F_j$. One obtains the reduced map

$$F^R(t_g)[\cdot] = \mathrm{tr}_{\rm TLF}\{F(t_g)[\cdot \otimes \rho_{\rm TLF}^{\rm eq}]\} \quad (8)$$

that only acts on the space of qubit density matrices. Standard factorized initial conditions are assumed with the TLF in equilibrium, $\rho_{\rm TLF}^{\rm eq}$. We use $\phi[F^R(t_g)]$ as fidelity for optimization in the relevant qubit subspace.

*Results and their discussion.*—In the above model we focus on optimizing controls for a $Z$-gate $\sigma_z$. This paradigmatic case demonstrates the virtues of our technique: (i) a gate error up to about 1 order of magnitude lower than the current optimal working point strategies; (ii) the gate error reaches the $T_1$ limit of the relaxation model; (iii) the optimized controls relate to optimal times via self-refocusing effects—showing how open systems GRAPE-derived controls provide physical insight in structured relaxation models. Similar findings are to be expected beyond single-qubit gates.

An overview of the accessible gate performance as a function of the duration $t_g$ of the gate is given in Fig. 1 (top). Excellent gate performance can be achieved for pulse time $t_g \gtrsim \pi/\Delta$. This corresponds to the static $\Delta\sigma_x$ inducing at least a full loop around $x$. Indeed, for the pulse at $t_g = 3.375/\Delta$ the evolution consists of a quarter $z$-rotation, a full loop around $x$, and the second quarter of the $z$ rotation leading to the total half rotation around $z$ necessary for the $Z$ gate; see the Bloch sphere in Fig. 2 (left) for a particular initial state. At shorter times the pulses cannot use the physical resource provided by the internal evolution to refocus the qubit.

At longer times the attainable gate performance mildly deteriorates, depending on the value of $\kappa$. This indicates that the optimal pulses are essentially limited by $T_1$ processes at the optimal working point. We compare the

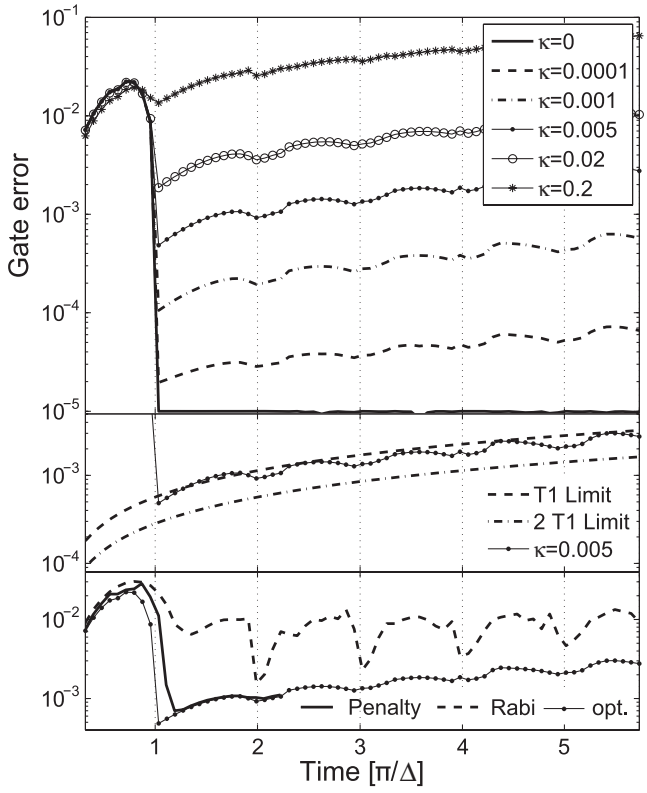


FIG. 1. Top: Gate error versus pulse time $t_g$ for optimal $Z$-gate pulses in the presence of a non-Markovian environment with dissipation strength $\kappa$. A periodic sequence of minima at around $t_n = n\pi/\Delta$ with $n \geq 1$ is obtained. Middle: The gate error of optimized pulses approaches a limit set by $T_1$ and $2T_1$, as shown with $\kappa = 0.005$. Bottom: Optimized pulses reduce the error rate by approximately 1 order of magnitude compared to Rabi pulses for $\kappa = 0.005$. Pulses starting from zero bias and with realistic rise times (penalty) require only slightly longer gate times, also for $\kappa = 0.005$. $E_2 = 0.1\Delta$, $\Lambda = 0.1\Delta$ and $T = 0.2\Delta$ in all panels.

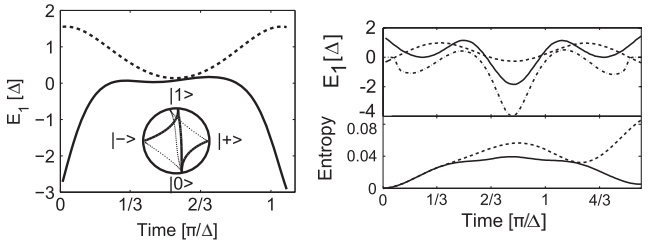


FIG. 2. Left: Rabi (dashed line) and optimized pulse (solid line) close to the optimal time at $t_g = 3.375/\Delta$ and $\kappa = 0.05$. Inset shows the evolution of initial state $\rho = |+\rangle\langle+|$, $|\pm\rangle = (|0\rangle \pm |1\rangle)/\sqrt{2}$ on the Bloch sphere under these pulses. Right: Comparison of pulse shape and qubit entropy between Rabi (dashed line), optimized (solid line), and penalty-constrained pulse ($- \cdot -$) at $t_g = 5.0/\Delta$ and $\kappa = 0.005$. $E_2 = 0.1\Delta$, $\Lambda = 0.1\Delta$, $T = 0.2\Delta$ in all panels.

performance to $1 - e^{-t_g/T_1}$ with $T_1$ obtained at $E_1 = 0$. The optimized pulses are able to beat this limit which indicates that $T_1(E_1 = 0)$ is a lower bound for the effective $T_1$; see Fig. 1 (middle panel). For clarity, we also compare to $1/e^{-t/T_{2,\min}}$ with $T_{2,\min} = 2T_1$.

Optimizing the qubit under decoherence can reduce the error by roughly 1 order of magnitude over conventional Rabi pulses, see Fig. 1 (bottom). The source of error of the Rabi pulses can be seen as the fast-oscillating counter-rotating component in the rotating frame, which is significant for these short, high-amplitude pulses consisting only of a few carrier periods. Only at certain times $t_n \simeq n\pi/\Delta$, $n \geq 1$, Rabi pulses perform well. At these $t_n$ one has $n$ rotations around $x$ due to the static field, refocusing the qubit. Further optimization gives moderate results: in the case $n = 2$ the errors are $(1 - \phi)_{\text{Rabi}} = 1.5 \times 10^{-3}$ and $(1 - \phi)_{\text{GRAPE}} = 0.9 \times 10^{-3}$. At other times, the pulse optimization redirects the $\Delta$ drift to refocus the TLF field and keeps the control at the optimal point $E_1 = 0$ as often as possible. As a result, the narrow and deep minima of the error for the regular Rabi pulse become shallow and broad using GRAPE.

Figure 2 (right) shows the control fields $E_1$ for a gate time $t_g = 5.0/\Delta$ and the respective time evolution of the entropy $-\text{Tr}\{\rho_q \ln \rho_q\}$, with $\rho_q$ the reduced qubit density matrix. The remaining qubit entropy at $t_g$ is significantly lower for the optimized pulse, but nonzero due to dissipation with $\kappa = 0.005$. Steep rises and offsets of pulses as in Fig. 2 can be smoothened by adding a penalty function to the fidelity $\tilde{\phi} = \phi - \int_0^{t_g} \alpha(t) E_1^2(t) dt$. A simple penalty kept constant for all iterations in the algorithm, $\alpha(t) = \alpha_0(2 - \tanh(\frac{t}{t_0}) + \tanh(\frac{t_g - t}{t_0}))$, was sufficient; see Fig. 2 (right). Here, the overall penalty and the characteristic rise-time parameter are chosen to be $\alpha_0 = 2.0/\Delta$ and $t_0 = 0.02/\Delta$, respectively. Figure 1 (bottom) shows that smooth pulses close to experimentally realistic settings come at a modest price of $0.5/\Delta$ in additional gate time. After $t_g \approx 3.75/\Delta$ the same gate errors as without the penalty function are obtained. Possible fast-oscillating components of the pulses could be eliminated by penalty functions in frequency space, which is beyond the scope of the present work.

We now analyze the dependence on the bath parameters. In Fig. 3 one can identify a nonmonotonic dependence of the error of the optimized pulse on $\gamma$. At low $\gamma$, one can approximate $(1 - \phi) = a + b\gamma$ (left inset). First, the linear growth with $\gamma$ accounts for the increasing probability for the TLF to flip at a random time during the evolution. This is reflected in the power spectrum of the RTN for low $\gamma$, where essentially $S(\omega \gg \gamma) \simeq \Lambda^2\gamma/\omega^2$, Eq. (5). For time-independent $E_1$ and very long evolution, $T_2$ would be dominated by $S(0)$ in the Markovian limit. However, at very fast manipulations through an external field, the environment is only sampled at higher frequencies, $1/t_g \sim \omega \gg \gamma$. Second, it turns out that $a \simeq 0$. This reflects that, for a static TLF ($\gamma = 0$) the GRAPE pulse fully compen-

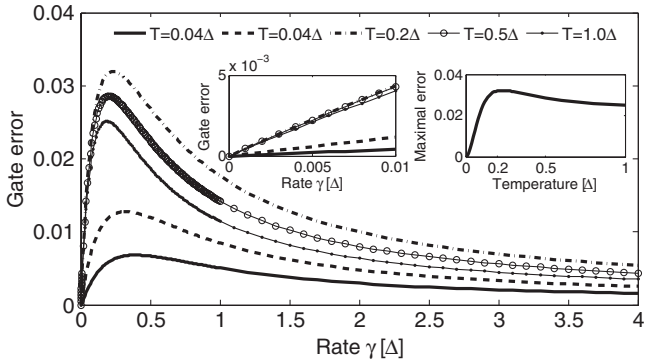


FIG. 3. Gate error versus TLF rate $\gamma$ at various temperatures for an optimized pulse with $t_g = 5.0/\Delta$. The left inset is a magnification of the low-$\gamma$ part of the main plot and reveals the linear behavior. The right inset shows the maximum of the curves of the main plot versus temperature. ($E_2 = 0.1\Delta$ and $\Lambda = 0.1\Delta$).

sates for the unknown initial state of the TLF. On the other hand, for a high flipping rate $\gamma$, the physics of motional narrowing sets in. This limits the low frequency noise and hence the decoherence to $S(\omega \ll \gamma) = \Lambda^2/\gamma$ which vanishes for $\gamma \to \infty$. Indeed, the high-$\gamma$ part of the error can be fitted by a law $c + d/\gamma$. The finite limiting value $c$ captures the residual decoherence which occurs even though the RTN model, Eq. (5), suggests absence of noise.

Consequently, there is a $\gamma_{\max}$ at which the error is maximum. Remarkably, $\gamma_{\max} \simeq 0.32\Delta \simeq \Delta/\pi$ independent of any other parameters such as temperature and pulse length: The attainable performance is worst if the TLF flips once per free rotation around $x$. The maximal error $(1 - \phi)(\gamma_{\max})$ as well as most other fit parameters show a nonmonotonic temperature dependence; see Fig. 3 (right inset). The maximal error is exponentially suppressed at low $T$ and saturates to a finite high-$T$ limit. The intermediate behavior can be related to the equilibrium susceptibility of the TLF, which is maximum at $k_B T \simeq 2E_2$. The more responsive the TLF is to perturbations of its $z$ field, the stronger it will influence the qubit.

*Conclusion.*—We have investigated an important model for decoherence in solid-state systems, a qubit coupled to a two-level fluctuator which itself is coupled to a heat bath. Our study is the first to exploit the explicit dynamics of a complex non-Markovian environment in optimal control of open systems for implementing quantum gates. For a wide range of parameters, we have identified self-refocusing effects, which are usually only visible at specific optimal pulse durations but can now be achieved more robustly. The pulses include offset and rise-time limitations of experimental settings. We have shown that both for fast and slow flipping of the TLF high-fidelity control can be achieved. The full qubit-fluctuator correlations turn out to be a crucial ingredient. The generality of our method can be harnessed for studies of multiqubit systems in the presence of a non-Markovian environment, such as multiple fluctuators, for instance.

We gratefully acknowledge support by NSERC discovery grants, by the EU in the projects EuroSQIP and QAP as well as by the DFG through SFB 631.

*rebentr@fas.harvard.edu
†fwilhelm@iqc.ca

[1] P. Bertet *et al.*, Phys. Rev. Lett. **95**, 257002 (2005).
[2] O. Astafiev *et al.*, Phys. Rev. B **69**, 180507(R) (2004).
[3] R. W. Simmonds *et al.*, Phys. Rev. Lett. **93**, 077003 (2004).
[4] A. Wallraff *et al.*, Nature (London) **431**, 162 (2004).
[5] D. Vion *et al.*, Science **296**, 886 (2002).
[6] T. Hayashi *et al.*, Phys. Rev. Lett. **91**, 226804 (2003).
[7] J. Clarke and F. K. Wilhelm, Nature (London) **453**, 1031 (2008).
[8] S. Jung *et al.*, Appl. Phys. Lett. **85**, 768 (2004).
[9] A. B. Zorin *et al.*, Phys. Rev. B **53**, 13 682 (1996).
[10] J. Eroms *et al.*, Appl. Phys. Lett. **89**, 122516 (2006).
[11] M. Steffen *et al.*, Phys. Rev. Lett. **97**, 050502 (2006).
[12] L. Faoro and L. Viola, Phys. Rev. Lett. **92**, 117905 (2004).
[13] H. Gutmann *et al.*, Phys. Rev. A **71**, 020302(R) (2005).
[14] G. Ithier *et al.*, Phys. Rev. B **72**, 134519 (2005).
[15] E. Collin *et al.*, Phys. Rev. Lett. **93**, 157005 (2004).
[16] N. Khaneja *et al.*, J. Magn. Reson. **172**, 296 (2005).
[17] T. Schulte-Herbrüggen *et al.*, Phys. Rev. A **72**, 042331 (2005).
[18] A. Spörl *et al.*, Phys. Rev. A **75**, 012302 (2007).
[19] T. Schulte-Herbrüggen *et al.*, arXiv:quant-ph/0609037.
[20] G. Gordon *et al.*, Phys. Rev. Lett. **101**, 010403 (2008).
[21] M. Möttönen *et al.*, Phys. Rev. A **73**, 022332 (2006); O.-P. Saira *et al.*, Phys. Rev. A **75**, 012308 (2007).
[22] S. Montangero *et al.*, Phys. Rev. Lett. **99**, 170501 (2007).
[23] H. Jirari and W. Pötz, Phys. Rev. A **74**, 022306 (2006).
[24] M. Grace *et al.*, J. Phys. B **40**, S103 (2007).
[25] D. J. Van Harlingen *et al.*, Phys. Rev. B **70**, 064517 (2004).
[26] P. Dutta and P. Horn, Rev. Mod. Phys. **53**, 497 (1981).
[27] M. Weissman, Rev. Mod. Phys. **60**, 537 (1988).
[28] R. T. Wakai and D. J. Van Harlingen, Phys. Rev. Lett. **58**, 1687 (1987).
[29] E. Paladino *et al.*, Phys. Rev. Lett. **88**, 228304 (2002).
[30] R. de Sousa *et al.*, Phys. Rev. Lett. **95**, 247006 (2005).
[31] A. Grishin *et al.*, Phys. Rev. B **72**, 060509(R) (2005); Y. M. Galperin *et al.*, Phys. Rev. Lett. **96**, 097009 (2006).
[32] R. Alicki *et al.*, Phys. Rev. A **73**, 052311 (2006).